Redox functionality mediated by adsorbed oxygen on a Pd oxide film over a Pd(100) thin structure: a first-principles study

2009 J. Phys.: Condens. Matter 21 485003

(http://iopscience.iop.org/0953-8984/21/48/485003)

J. Phys.: Condens. Matter **21** (2009) 485003 (7pp) doi:10.1088/0953-8984/21/48/485003

Redox functionality mediated by adsorbed oxygen on a Pd oxide film over a Pd(100) thin structure: a first-principles study

K Kusakabe[1], K Harada[2], Y k Ikuno[1] and H Nagara[1]

[1] Graduate School of Engineering Science, Osaka University, 1-3 Machikaneyama-cho, Toyonaka, Osaka 560-8531, Japan
[2] Institute for Solid State Physics, University of Tokyo, Kashiwanoha, Kashiwa, Chiba 277-8581, Japan

E-mail: kabe@mp.es.osaka-u.ac.jp

Received 11 June 2009, in final form 24 September 2009
Published 30 October 2009
Online at stacks.iop.org/JPhysCM/21/485003

Abstract
Stable oxygen sites on a PdO film over a Pd(100) thin structure with a $(\sqrt{5} \times \sqrt{5})$R27° surface unit cell are determined using the first-principles electronic structure calculations with the generalized gradient approximation. The adsorbed monatomic oxygen goes to a site bridging two twofold-coordinated Pd atoms or to a site bridging a twofold-coordinated Pd atom and a fourfold-coordinated Pd atom. Estimated reaction energies of CO oxidation by reduction of the oxidized PdO film and N_2O reduction mediated by oxidation of the PdO film are both exothermic. Motion of the adsorbed oxygen atom between the two stable sites is evaluated using the nudged elastic band method, where an energy barrier for a translational motion of the adsorbed oxygen may become ∼0.45 eV, which is low enough to allow fluxionality of the surface oxygen at high temperatures. The oxygen fluxionality is allowed by the existence of twofold-coordinated Pd atoms on the PdO film, whose local structure has a similarity to that of Pd catalysts for the Suzuki–Miyaura cross-coupling. Although NO_x (including NO_2 and NO) reduction is not always catalyzed by the PdO film only, we conclude that continual redox reactions may happen mediated by oxygen-adsorbed PdO films over a Pd surface structure, when the influx of NO_x and CO continues, and when the reaction cycle is kept on a well-designed oxygen surface.

1. Introduction

Oxidation and reduction processes on palladium surfaces are attracting interest, since the understanding of catalytic reactions on palladium is a key point to explore the functionality of this solid catalyst working as a three-way catalyst for automotive emissions control [1]. When oxidation of Pd proceeds, various stable Pd oxide films are created to cover the Pd surface, depending on the surface morphology [2]. A stable surface structure of an oxidized Pd(100) surface is known to be a $(\sqrt{5} \times \sqrt{5})$R27° PdO monolayer [3, 4]. Formation of a PdO thin film stabilizes the Pd(100) surface against further oxidation. Interestingly, catalytic reactivity is often attributed to surface oxides [5, 6]. Here, two questions arise. Is there a process to reach the oxidation of the Pd substrate below the PdO film? How high is the reactivity of the PdO film itself in a catalytic reaction process?

In a study of CO oxidation at Pd(100), Rogal *et al* have shown a surface phase diagram in constrained thermodynamic equilibrium obtained using first-principles statistical mechanics [7]. They carefully constructed the phase diagram with converged slab structures with surfaces reacted with oxygen and/or CO. Interestingly, no co-adsorption structures on Pd(100) in equilibrium was found. But Langmuir–Hinshelwood reaction processes were expected around the phase boundary between the surface oxide phases and CO-adsorbed surfaces. In their surface phase diagram, we can see a wide stable phase of $(\sqrt{5} \times \sqrt{5})$R27° surface oxide structure, which was found in the experiments.

In consideration of the three-way catalysts, CO oxidation happens continually in a reactor by gas flow. Thus, one needs to consider the reactivity of the catalyst in a low partial pressure of CO. A key to understand total reactivity under this condition may be found in that, on a three-way catalyst

material, other surface structures coexist with a Pd surface. The phase diagram of Rogal suggests that surface oxide formation without any extra adsorbents on the Pd oxide film is favored in a wide pressure range. Here, we may start from re-considering reactivity of surface oxides in a non-equilibrium condition with a fluctuating density of surface oxygen. There, adsorbed oxygen atoms might come from a catalytic material structure other than the PdO film. Since it is a hard task to treat all the possibilities, we just consider a single adsorbed oxygen atom assumed to be provided by other surfaces of the catalytic material than the PdO film and test its stability and reactivity. Fluctuating behavior of the surface oxygen will be called fluxionality. For this possible motion of oxygen atoms, morphological softness is preferable. If this character is expected in nanometer-scale Pd structures, the condition to have fluxionality may be relaxed. Thus, we should also search for a simulation result which might open our eyes.

To study reactivity of the $(\sqrt{5} \times \sqrt{5})$R27° PdO film on a Pd(100) surface, we performed first-principles structural optimization simulations to obtain stable oxygen-adsorbed structures of the PdO thin film. Slab models of PdO/Pd(100) were used for the simulation and thus the calculation data should be interpreted as results for a thin Pd structure with an oxidized surface. Two stable sites were found in this study. The stability of these sites depends on the local atomic configuration of the whole Pd oxide structure in the simulation. The choice of the structure of the thin Pd substrate even relaxes conditions for possible oxygen migration. We evaluated reaction energies of reduction processes for NO_x (NO, NO_2 or N_2O) and a CO oxidation process to estimate functionality of the PdO surface as a redox catalyst. Characteristic features of the adsorbed reactive oxygen atom are explored by analyzing the local electronic density of states and barrier heights of oxygen migration. The estimated transition path of the oxygen atom reveals that there can exist fluxionality analogous to motions of fluxional function groups in molecules [8] and clusters. Finally, we will summarize our conclusions, in which an expected mechanism of the catalytic function is proposed.

2. Methods of calculations

A generalized gradient approximation [9, 10] based on the density functional theory [11, 12] was adopted in our calculation. The calculation was done using the plane-wave expansion with the ultra-soft pseudopotentials [13] realized in the Quantum-espresso version 3.2.3 package [14]. Conditions for the simulation were the following. Cutoff energies for the wavefunction and the charge density were 408 eV and 2721 eV, respectively. The k-point sampling was done with $8 \times 8 \times 1$ mesh points in the first Brillouin zone.

As a typical model structure, we consider a slab model which consists of a PdO film on two Pd layers. We call this 'model I' or 'the thin model'. This model is very thin. We will show that some characteristic properties of the PdO film on this thin Pd layer are qualitatively different from those of the PdO film on the stable Pd(100) surface, although its structure is only slightly different from that of the PdO on the stable Pd (100) surfaces. The structure of model I gives us an interesting result on the oxygen fluxionality. We compare the result with another structure with a PdO film on up to five Pd sublayers, which we call 'model II' or 'the thick model'. The thickness of the Pd layers of model II is enough to reproduce the PdO film structure on the Pd(100) surface, since we have the converged PdO structure for three, four or five Pd layers as substrates.

Table 1. Optimized structural parameters of the PdO film in model I (two Pd layers below the PdO film) (upper half of the table) and model II (four Pd layers below the PdO film) (lower half of the table). The coordinates x and y are in-plane coordinates, while Δz gives a shift in a vertical structural parameter from the center of z coordinates of Pd atoms in the PdO layer.

	x (Å)	y (Å)	Δz (Å)
Pd	3.916	2.976	−0.052
Pd	1.020	5.182	0.238
Pd	−1.720	3.882	0.198
Pd	1.346	1.448	−0.384
O	0.248	3.292	−0.369
O	2.976	4.774	−0.473
O	−0.846	5.560	1.066
O	1.885	6.916	1.012
Pd	3.932	3.046	−0.040
Pd	1.120	5.192	0.100
Pd	−1.642	3.840	0.095
Pd	1.195	1.618	−0.155
O	0.275	3.403	−0.531
O	3.042	4.808	−0.533
O	−0.764	5.548	0.761
O	1.965	6.924	0.781

To check the validity of the simulation for model I, we performed several test simulations. A repeated slab model with a vacuum layer of 7 Å thickness was employed for each simulation. Convergence is seen as follows. When the thickness of the vacuum layer is increased from 7 to 15 Å, atomic positions changed only slightly with an absolute error of less than 10^{-4} Å. The total energy changes only less than 7×10^{-3} eV for model I.

For the structural optimization of model II, we prepared the PdO structure of a surface unit cell of $(\sqrt{5} \times \sqrt{5})$R27° above three, four or five atomic layers of Pd, which is a structure with up to five Pd sublayers. At the start of the simulations, the size of the surface unit cell of the PdO was set so that the lattice constants of the Pd sublattice are equal to the lattice constants of an equilibrium lattice of the bulk Pd and kept fixed in each optimization calculation. All of the relative atomic positions are relaxed in each simulation. The optimized structures reproduce the former result [4] qualitatively and almost quantitatively (see table 1 and also the discussion in the final paragraph of section 5).

However, when we look at model I, the PdO film showed a structure little modified from that of model II. For the comparison, we summarize the optimized structural parameters of models I and II in table 1. We note here that the distances between Pd layers are: $d_{\mathrm{PdO-Pd_2}} = 2.6773$ Å and $d_{\mathrm{Pd_2-Pd_3}} = 2.0869$ Å for model I and $d_{\mathrm{PdO-Pd_2}} = 2.5464$ Å, $d_{\mathrm{Pd_2-Pd_3}} = 2.0529$ Å, $d_{\mathrm{Pd_3-Pd_4}} = 2.0526$ Å, $d_{\mathrm{Pd_4-Pd_5}} = 2.0517$ Å and $d_{\mathrm{Pd_5-Pd_6}} = 2.0226$ Å for model II, where Pd_i with $i = 2, 3, \ldots, 6$ represents the ith Pd sublayer which consists of up to five substrate layers.

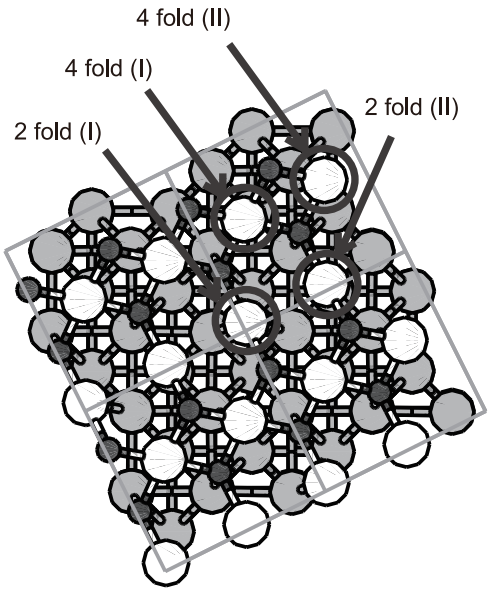

Figure 1. The optimized $(\sqrt{5} \times \sqrt{5})$R27° PdO film on Pd(100) surface of model I obtained by the present simulation. White spheres are Pd atoms in the PdO film, bright gray spheres are Pd atoms in the substrate and dark gray spheres are oxygen atoms. Each square represents a unit cell. In a unit cell, there are two fourfold-coordinated sites and two twofold-coordinated sites of Pd atoms, which are marked by circles.

The structure shown in figure 1 is an optimized structure of model I, which was obtained by structural optimization, in which the interatomic forces were reduced to less than 1.3×10^{-5} eV au^{-1}. In the optimized film structure, fourfold-coordinated sites and twofold-coordinated sites of Pd exist as depicted in figure 1. Existence of the twofold-coordinated Pd atoms is important for our discussion.

3. Optimized structures of oxygen-adsorbed PdO films

Each simulation for the determination of the oxygen adsorbed site was started from the optimized structure of the PdO thin film shown in section 2. At first, we prepared four different initial structures using model I. A single atomic oxygen was put on a Pd atom in the topmost oxidized layer and then the position of the oxygen as well as the surface atomic structure was optimized. Note that we have four distinct Pd sites in the unit cell of the $(\sqrt{5} \times \sqrt{5})$R27° structure. We performed four simulations to optimize the oxygen-adsorbed film structure and we obtained two stable structures.

The obtained structures for adsorption of an oxygen atom per each surface unit cell of $(\sqrt{5} \times \sqrt{5})$R27° PdO are shown in figures 2 and 3. The first one has an oxygen atom at a bridge site (figure 2), in which the adsorbed oxygen bridges two Pd atoms in the twofold coordination. The other has an oxygen atom at another bridge site (figure 3), in which the adsorbed oxygen atom has bond connections with a Pd atom in the twofold coordination and another Pd atom in the fourfold coordination. We call the former site bridge site (I) and the latter site bridge site (II). In the bridge site (II) structure, a

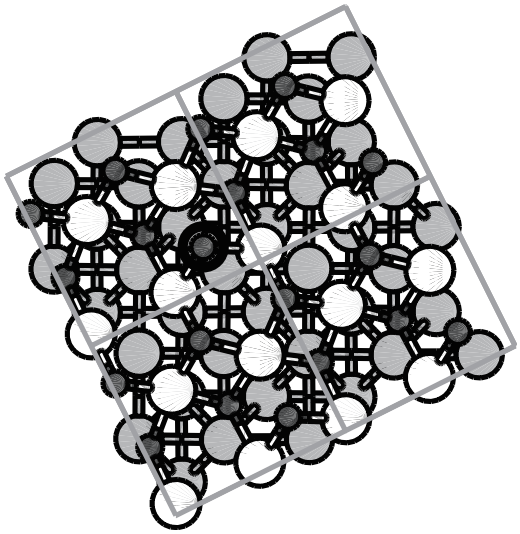

Figure 2. The atomic configuration of the bridge site (I) structure. The adsorbed oxygen (O1) shown by a circle connects two twofold-coordinated Pd atoms.

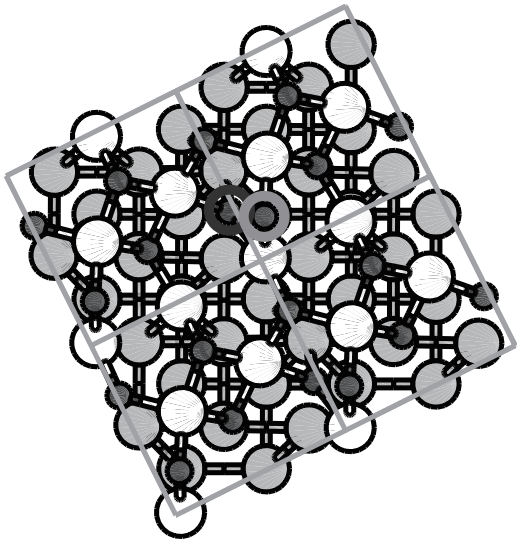

Figure 3. The atomic configuration of the bridge site (II) structure. The adsorbed oxygen shown by a bright circle connects a twofold-coordinated Pd atom and a fourfold-coordinated Pd atom. Another oxygen atom, which formed the PdO film before the optimization, and is shown by a dark circle, has new bond connections with Pd atoms in the second Pd layer.

surface oxygen atom which had a bond connection with the two Pd atoms changes its bond connections: one of the bond connections is cut through the oxygen adsorption and a new bond with a Pd atom in the second Pd layer is created. Thus, the subsurface oxidation happens in this process of monatomic oxygen adsorption.

To confirm the subsurface oxidation, we evaluated the Löwdin charges. A value on a Pd atom in the second layer changes from 9.8995 to 9.7614 when the position of the adsorbed oxygen changes from bridge site (I) to bridge site (II). The value of ∼9.75 is obtained when the Pd atom has a bond connection with oxygen in a PdO film. Thus we can say

Table 2. Reaction energy of NO_x reduction and CO oxidation on $(\sqrt{5}\times\sqrt{5})$R27° PdO/Pd(100). Definition of each energy is given by ΔE in the text.

Oxygen sites	NO_2 reduction energy (eV)	NO reduction energy (eV)	N_2O reduction energy (eV)	CO oxidation energy (eV)
Bridge (I)	−0.194	0.007	0.613	2.775
Bridge (II)	−0.403	−0.097	0.561	2.827

Table 3. Adsorption energy of O and O_2 on $(\sqrt{5}\times\sqrt{5})$R27° PdO/Pd(100). The energy is per the surface unit cell.

Oxygen sites	O adsorption energy (eV)	O_2 adsorption energy (eV)
Bridge I	2.255	−0.069
Bridge II	2.202	−0.121

that the subsurface oxidation proceeds through the formation of the bridge site (II) structure in model I.

We now compare the total energy of the two solutions. The former bridge site (I) is energetically favorable by 52.2 meV compared to the latter bridge site (II). Bridge site (I) is a natural structure, since the adsorbed oxygen atom forms bond connections with two twofold-coordinated Pd atoms. In a unit cell, there are two bridge sites (I). As discussed later, we will find a migration path of an oxygen atom going from one bridge site (I) to the other bridge site (I).

Bridge site (II) may be regarded as an intermediate step in the subsurface oxidation. A surface oxygen atom originally forming a bond in the PdO top layer approaches a Pd atom in the second Pd layer, forming a new bond connection with it. The adsorption energy is a little larger for bridge site (I) than that of bridge site (II). This result also suggests that the reaction of subsurface oxidation does not easily occur.

Next, we tried to find these two bridge sites using model II. In this thick model, however, we could not find bridge site (II). Even if we started the optimization of the adsorbed oxygen located approximately at a position of bridge site (II), it went to bridge site (I). Another simulation searching for an oxygen migration path from one bridge site (I) to another bridge site (I) did not show any structure similar to the bridge site (II) structure in the path. Thus, we concluded that bridge site (II) is found only in model I with the very thin Pd substrate in the nanometer scale.

4. Estimation of reaction energy

To estimate the reaction energy ΔE of NO_x reduction and CO oxidation, we consider the next reaction paths. The former depends on the species of NO_x:

$$2x\,(\mathrm{PdO})_4/\mathrm{Pd} + 2\mathrm{NO}_x \rightarrow \mathrm{N}_2 + 2x\,(\mathrm{PdO})_4\mathrm{O}/\mathrm{Pd}.$$

This process may occur when NO_x molecules dissociate on the PdO surface and oxygen atoms stay on the surface. However, we do not exclude other complex reaction paths. If NO_x molecules dissociate on another catalytic oxide surface, and if the adsorbed oxygen atoms move to the PdO surface, the process is effectively realized. The reaction energy is estimated by the following energy difference:

$$\Delta E = 2x\,E_{\mathrm{PdO}} + 2E_{\mathrm{NO}_x} - 2x\,E_{\mathrm{PdO+O}} - E_{\mathrm{N}_2}.$$

The latter CO oxidation due to the adsorbed oxygen atoms may be given in the next reaction process in the Eley–Rideal reaction scheme (the ER scheme):

$$(\mathrm{PdO})_4\mathrm{O}/\mathrm{Pd} + \mathrm{CO} \rightarrow \mathrm{CO}_2 + (\mathrm{PdO})_4/\mathrm{Pd}.$$

The reaction energy is estimated as follows:

$$\Delta E = E_{\mathrm{PdO}} + \mathrm{O} + E_{\mathrm{CO}} - E_{\mathrm{PdO}} - E_{\mathrm{CO}_2}.$$

Here, the energy of a molecule is given by a simulation with the same supercell as that utilized in simulations of $(PdO)_4$/Pd and $(PdO)_4$O/Pd.

The reaction energy is summarized in table 2 for NO_2, NO, N_2O and CO. When the value is positive, the reaction is exothermic. The result suggests that N_2O may dissociate on PdO surfaces and that the adsorbed oxygen is reactive with CO. Although the reduction of NO_2 only by oxidation of the PdO film is endothermic, the absolute value of the reaction energy is 7% of the CO oxidation energy for bridge site (I). Considering a successive reaction of NO_x reduction and CO oxidation on $(\sqrt{5}\times\sqrt{5})$R27° PdO, we conclude that an exothermic process $2\mathrm{NO}_x + 2x\mathrm{CO} \rightarrow \mathrm{N}_2 + 2x\mathrm{CO}_2$ is favored at an optimized condition of the temperature and the partial pressures of gas components.

To examine the possibility on reaction paths, values of the adsorption energy of O_2 and O were obtained. The evaluation is given by determining the following energy difference:

$$\mathrm{O} + (\mathrm{PdO})_4/\mathrm{Pd} \rightarrow (\mathrm{PdO})_4\mathrm{O}/\mathrm{Pd},$$

$$\Delta E = E_{\mathrm{PdO}} + E_{\mathrm{O}} - E_{\mathrm{PdO+O}},$$

$$\tfrac{1}{2}\mathrm{O}_2 + (\mathrm{PdO})_4/\mathrm{Pd} \rightarrow (\mathrm{PdO})_4\mathrm{O}/\mathrm{Pd},$$

$$\Delta E = E_{\mathrm{PdO}} + \tfrac{1}{2}E_{\mathrm{O}_2} - E_{\mathrm{PdO+O}}.$$

The result shown in table 3 suggests that O_2 molecules in a gas phase do not spontaneously react with the PdO film. Thus we cannot expect dissociative adsorption of O_2 on this Pd oxide surface. But, if we have atomic oxygen, its reactivity with the PdO film is enough high. If we have a chance to obtain this active atomic oxygen from dissociative adsorption of NO_x somewhere on the catalyst surface, the three-way catalytic reaction would work smoothly. At the same time, we should consider this oxygen-adsorbed PdO film as an intermediate structure of the whole catalytic process.

5. Surface migration of adsorbed oxygen

It is well known that the NO_x reduction process consists of a complex process with multiple reaction paths [15]. In our

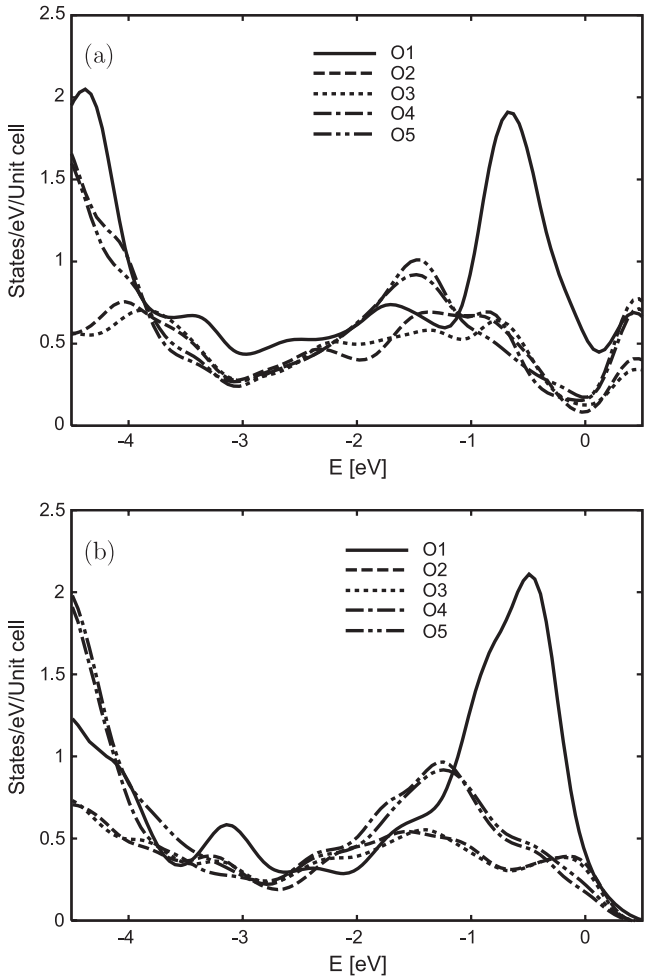

Figure 4. The projected local density of states at oxygen sites in the bridge site (I) structure for (a) model I and (b) model II. The projection is done using oxygen p orbitals. The adsorbed oxygen denoted as O1 is at bridge sites (I). Other oxygen atoms (O2 $\cdots$ O5) are those in a unit cell of the PdO film. The origin of the energy is the Fermi energy.

discussion, we assume that an oxygen-adsorbed PdO/Pd(100) surface can be an intermediate state of a total redox reaction. To explore all possible processes on the oxygen-adsorbed surfaces, we need to have information on every reaction path and its activation barrier. This problem needs rather detailed simulations. To test the functionality of the oxygen-adsorbed oxide film as a catalyst, however, we can confirm the reactivity of the adsorbed oxygen atom.

A first clue of finite reactivity of the adsorbed oxygen is local information on the electronic structure. We obtained the local density of states (LDOS) given by our GGA simulation. (figure 4) The data is given by projecting only the contribution of p orbitals at each oxygen atom. Comparison of data on each oxygen atom reveals that the monatomic adsorbed oxygen at bridge site (I) has an enhancement in LDOS at around the Fermi energy. Thus we can conclude that the oxygen has a frontier orbital [16] and the reactivity is enhanced at this oxygen site.

This oxygen adatom with high reactivity has further mobility on this surface. To check possible fluxionality of the oxygen adatom, we performed an estimation of a migration path from bridge site (I) to bridge site (II) for model I, and from bridge site (I) to the next bridge site (I) for model II. The nudged elastic band method (NEBM) [17] is adapted for this simulation. Seven replicas for model I and eight replicas for model II were prepared and the paths were optimized. Some snapshots in between these stable sites are shown in figure 5.

The barrier height for this transition of model I is estimated to be $\simeq$0.45 eV. Optimization of the atomic configuration of the PdO film is important to have this value. Gradual modification of the PdO structure is seen in panels (b) and (c) of figure 5. In this transition, the adsorbed oxygen keeps a bond connection with a twofold-coordinated Pd atom in the PdO film. We can interpret that a rotational motion of the extra oxygen atom around a O–Pd–O structure occurs at the twofold-coordinated Pd site in the PdO film. Thus, the existence of low-coordinated Pd atoms is a key to understand possible fluxionality of the adsorbed oxygen.

We determined the first barrier of 0.45 eV for the possible total transition from a stable bridge site (I) structure to another bridge site (I) structure in model I. We have another barrier from the bridge site (II) structure of figure 5(d) to another bridge site (I). However, it is much smaller than the above barrier, since the next bridge site (I) structure is easily accessible from the bridge site (II) structure. There might be a direct path from one bridge site (I) to another bridge site (I), but the barrier height should be a little higher than the above value. Thus, we assume that a typical barrier height is around 0.45 eV for the migration of oxygen atoms on PdO of the thin model (see figure 6).

A simulation for model II tells us another picture. We performed an NEBM simulation from the bridge site (I) structure to another neighboring bridge site (I) structure using model II. In this simulation, the barrier height is found to be $\sim$1.1 eV. There appears to be no bridge site (II) structure in this process. In addition, we found that the local structure of the substrate was almost kept rigid in the reaction path, although all of the atoms were allowed to move. This rigidity prevents modification of the PdO film. If continual bond formations between the adsorbed oxygen and Pd atoms on the path appear, the height of the energy barrier decreases. But, in this model II, the energy reduction hardly occurs. In contrast, the easiness of morphological change in the structure allows easy fluxionality of oxygen in model I. Thus, we conclude that the fluxionality may be attributed to a nanometer-scale thin oxidized Pd structure.

The value of 0.45 eV for the barrier is rather small. If we refer to values in table 2, we can expect a large kinetic energy of the adsorbed oxygen atoms coming from the reaction heat of NO_x reduction. The oxygen atoms will move approximately with a motional energy of typically $\sim$1 eV. Thus, the mobility of oxygen atoms would be easily retained in the whole process.

Here, we should note that known PdO films on various Pd surfaces always have twofold-coordinated sites as well as PdO_4 units [5, 6]. We can thus hope to have similar migration paths of oxygen around the twofold-coordinated Pd atoms. Here, the bond angle of a O–Pd–O structure shows a notable difference between model I and model II. In model I, the O–Pd–O angles

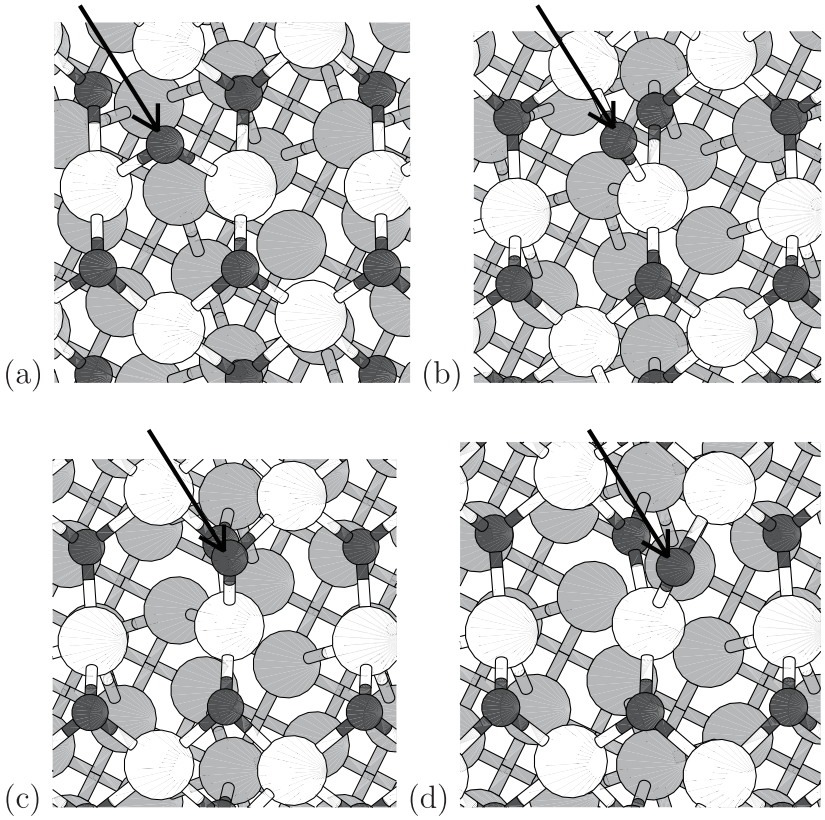

Figure 5. Atomic structure of oxygen adsorbed on the PdO film in a transition path from the bridge site (I) structure (a) to the bridge site (II) structure (d) in model I. The third and the fifth structures in a total of seven replicas are shown in (b) and (c), respectively. The adsorbed oxygen marked by an arrow keeps a bond connection always with the twofold-coordinated Pd atom at the center in each panel.

are 135° and 160°, while the values increase and become 162° and 169° in model II. The latter values are approximately equal to 170° found in the literature [4]. The bond angle itself does not directly reflect the migration barrier. However, small angles in O–Pd–O happen only for model I, where relaxation in the PdO film structure is easily achieved. Thus the value of the migration barrier should reflect this structural feature, i.e. easy structural modification. Once the fluxionality of reactive oxygen is guaranteed owing to this feature, we will have an enhanced cross section for the CO oxidization process. But, we should note again that the structural feature of model I is lost already for a slab model with three or more Pd layers in the substrate.

6. Summary and conclusions

We have obtained two stable structures for an oxygen-adsorbed PdO film over a Pd(100) thin structure. The existence of both twofold-coordinated Pd atoms and fourfold-coordinated Pd atoms is important to have fluxionality of oxygen atoms at stable bridge sites (I). The oxygen atom moves around a twofold-coordinated Pd atom, which is a characteristic feature of the PdO films. On a PdO film formed on a substrate of two Pd layers, the oxygen atom may reach a bridge site (II). In this case, the migration barrier may be reduced to ∼0.45 eV. Because half of the Pd atoms in the PdO film are twofold-coordinated and can provide adsorption sites for the activated oxygen atoms, the fluxionality of oxygen can happen on the whole PdO film structure.

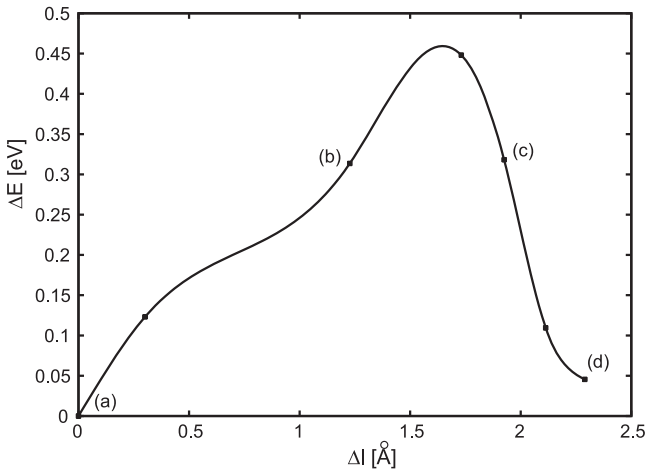

Figure 6. Oxygen migration barrier from bridge site (I) to bridge site (II) in model I. The horizontal axis is given by the distance between a twofold-coordinated Pd and the active oxygen atom. This distance becomes the Pd–O bond length of the adsorbed oxygen and a twofold-coordinated Pd atom in the PdO film. The origin of the value, Δl, is shifted by the bond length in the stable bridge site (I). The vertical axis represents a migration energy. Structures given by figures 5(b) and (c) are around $\Delta l = 1.2$ and 1.9, respectively.

Because of enhancement in the reactivity estimated by LDOS and fluxionality in migration paths as well as the

exothermic nature in a continual reaction of CO oxidation and N_xO reduction, we conclude that continual redox reactions may occur through the motion and reaction of active oxygen atoms on the stable PdO film.

Now, we have a well-defined picture of catalytic reactions of the PdO surfaces with the twofold-coordinated Pd atom surrounded by two oxygen atoms. Here, we should note that the local structure of this O–Pd–O bond connections is similar to those found in Pd catalysts [18] utilized for the C–C cross-coupling reactions of the Suzuki–Miyaura coupling, [19] where the ligands might be phosphine or arsine, rather than oxides. We can expect that the O–Pd–O structure is reactive also for the hydrocarbon structures as in homogeneous catalysts. Since the redox reactivity for the NO_x and CO mixture is energetically confirmed as above, we can also expect to have a finite reactivity for the heterogeneous catalysts even in a three-way catalytic reaction.

When we notice that the above mechanism found in the PdO film can be a general one, we have an idea to find similar reactive surfaces in oxide films. Oxide films with low-coordinated metal atoms in an oxide structure provide fluxionality of the adsorbed oxygen atoms as found in the PdO film. In particular, twofold-coordinated metal atoms can have important roles. If an attached extra oxygen atom rotates around the twofold-coordinated metal, the oxygen can easily move around on the film by passing from one stable oxygen state to the others. When a CO molecule in the gas phase collides with the adsorbed oxygen atom in the highly reactive state, the reaction in the ER scheme happens. If the oxygen is in a fluxional state, reaction rates are inevitably increased, because the cross section of the collision should be enhanced. The ER scheme is unlikely to be sensitive to the surface temperature, which would be necessary for a solid catalyst effective in a wide temperature range.

For a continual reaction, to keep the low coordination of metal atoms in surface oxides is thus the key factor. In order to have this functionality, the following conditions may be needed for a catalytic oxide.

(i) Existence of fluxionality for oxygen motion around a low-coordinated metal atom.
(ii) Prevention of highly oxidized state at catalytic sites to keep the low coordination.
(iii) Prevention of over-reduction at catalytic sites to keep the oxide structure.
(iv) Existence of a buffer for oxygen atoms in the catalyst or in the environment.

The first point ensures high reactivity of the CO reduction process. It also relates to reactivity of NO_x reduction, since mobility of the extra oxygen allows the catalyst also to keep a reaction rate of NO_x reduction. The second point is required to keep the reaction site active. This factor might be much more easily achieved, if we have another metal species which is much more easily oxidized and if the species form a buffer of oxygen atoms inside a catalytic structure. The third factor is important to prevent an aging effect, where so-called agglomeration of metal particles kills the redox functionality.

To preserve the reactive property, the oxygen buffer would be effective. The buffer may be a part of the whole catalyst structure, i.e. the substrate. It should be less reductive than Pd, since oxygen atoms should be kept in the buffer under the over-reduction environment. For this purpose, a pure metal substrate is less effective. Existence of rare-earth elements in an oxide structure, for example, would be important for this function.

Thus realization of the low-coordinated oxide film structures even in another bulk oxide structure can be the final answer for a highly reactive redox catalyst. The oxide support is actually often used in a real three-way catalyst. If we look at the functionality of the perovskite catalyst [1, 20], the present mechanism may work as a hidden important ingredient enhancing the performance.

Acknowledgments

The authors thank all of the research members in the Elements Science and Technology Project entitled ‘New development of self-forming nano-particle catalyst without precious metals’. One of the authors (KK) is grateful for discussions with Professors Y Tobe and K Fukui. This work was supported by the Elements Science and Technology Project and also by Grants-in-Aid for Scientific Research in Priority Areas (nos. 17064006 and 19051016) and a Grant-in-Aid for Scientific Research (no. 19310094). The computation is partly done using the computer facility of ISSP, University of Tokyo.

References

[1] Nishihata Y, Mizuki J, Akao T, Tanaka H, Uenishi M, Kimura M, Okamoto T and Hamada N 2002 *Nature* **418** 164
[2] Mittendorfer F, Seriani N, Dubay O and Kresse G 2007 *Phys. Rev.* B **76** 233413
[3] Todorova M *et al* 2003 *Surf. Sci.* **541** 101
[4] Kostelník P, Seriani N, Kresse G, Mikkelsen A, Lundgren E, Blum V, Šikola T, Varga P and Schmid M 2007 *Surf. Sci.* **601** 1574
[5] Klikovits J, Napetschnig E, Schmid M, Seriani N, Dubay O, Kresse G and Varga P 2007 *Phys. Rev.* B **76** 045405
[6] Westerström R *et al* 2007 *Phys. Rev.* B **76** 155410
[7] Rogal J, Reuter K and Scheffler M 2007 *Phys. Rev. Lett.* **98** 046101
[8] von W, Doering E and Roth W R 1963 *Angew. Chem. Int. Edn Eng.* **2** 115
[9] Perdew J P, Burke K and Ernzerhof M 1996 *Phys. Rev. Lett.* **77** 3865
[10] Perdew J P, Burke K and Ernzerhof M 1997 *Phys. Rev. Lett.* **78** 1396
[11] Hohenberg P and Kohn W 1964 *Phys. Rev.* **136** B864
[12] Kohn W and Sham L J 1965 *Phys. Rev.* **140** A1133
[13] Vanderbilt D 1990 *Phys. Rev.* B **41** 7892
[14] Giannozzi P *et al* 2009 *J. Phys.: Condens. Matter* **39** 395502
[15] Kondratenko E V and Pérez-Ramírez J 2003 *Catal. Lett.* **91** 211
[16] Fukui K, Yonezawa T and Shingu H 1952 *J. Chem. Phys.* **20** 722
[17] Mills G, Jónsson H and Schenter G K 1994 *Surf. Sci.* **324** 305
[18] Hayashi T, Konishi T, Kobori T, Kumada T, Higuchi T and Hirotsu T 1984 *J. Am. Chem. Soc.* **106** 158
[19] Miyaura N and Suzuki A 1979 *J. Chem. Soc. Chem. Commun.* 866
[20] Tanaka H, Tan I, Uenishi M, Kimura M and Dohmae K 2001 *Top. Catal.* **16/17** 63